HHS Public Access

Author manuscript

Exp Eye Res. Author manuscript; available in PMC 2016 November 01.

Published in final edited form as:

Exp Eye Res. 2015 November ; 140: 94–105. doi:10.1016/j.exer.2015.07.022.

Systemic Treatment with a 5HT1a Agonist Induces Anti-oxidant Protection and Preserves the Retina from Mitochondrial Oxidative Stress

Manas R. Biswal[1,2], **Chulbul M. Ahmed**[1,2], **Cristhian J. Ildefonso**[1], **Pingyang Han**[1], **Hong Li**[1], **Hiral Jivanji**[1], **Haoyu Mao**[1], and **Alfred S. Lewin**[1]

[1]Department of Molecular Genetics and Microbiology, University of Florida College of Medicine, Box 100266, Gainesville, FL, 32610-0266 USA

Abstract

Chronic oxidative stress contributes to age related diseases including age related macular degeneration (AMD). Earlier work showed that the 5-hydroxy-tryptophan 1a (5HT1a) receptor agonist 8-hydroxy-2-(di-n-propylamino)-tetralin (8-OH-DPAT) protects retinal pigment epithelium (RPE) cells from hydrogen peroxide treatment and mouse retinas from oxidative insults including light injury. In our current experiments, RPE derived cells subjected to mitochondrial oxidative stress were protected from cell death by the up-regulation of anti-oxidant enzymes and of the metal ion chaperon metallothionein. Differentiated RPE cells were resistant to oxidative stress, and the expression of genes for protective proteins was highly increased by oxidative stress plus drug treatment. In mice treated with 8-OH-DPAT, the same genes (*MT1*, *HO1*, *NqO1*, *Cat*, *Sod1*) were induced in the neural retina, but the drug did not affect the expression of *Sod2*, the gene for manganese superoxide dismutase. We used a mouse strain deleted for *Sod2* in the RPE to accelerate age-related oxidative stress in the retina and to test the impact of 8-OH-DPAT on the photoreceptor and RPE degeneration developed in these mice. Treatment of mice with daily injections of the drug led to increased electroretinogram (ERG) amplitudes in dark-adapted mice and to a slight improvement in visual acuity. Most strikingly, in mice treated with a high dose of the drug (5 mg/kg) the structure of the RPE and Bruch's membrane and the normal architecture of photoreceptor outer segments were preserved. These results suggest that systemic treatment with this class of drugs may be useful in preventing geographic atrophy, the advanced form of dry AMD, which is characterized by RPE degeneration.

1. Introduction

Clinical and biochemical data implicate oxidative stress in the pathogenesis of age related macular degeneration (AMD) (Cano, Thimmalappula, Fujihara, Nagai, Sporn, Wang,

Correspondence to: Alfred S. Lewin.

[2]These authors contributed equally to this paper.

Conflicts of Interest: This project was supported by Alcon Laboratories, now a part of Novartis Pharmaceuticals.

Neufeld, Biswal and Handa, ;Hollyfield, Bonilha, Rayborn, Yang, Shadrach, Lu, Ufret, Salomon and Perez, 2008;Jarrett and Boulton, 2012;Shen, Dong, Hackett, Bell, Green and Campochiaro, 2007). Tobacco use, which exposes both the smoker and bystanders to high levels of oxidants, is the biggest environmental risk factor for AMD (Smith, Assink, Klein, Mitchell, Klaver, Klein, Hofman, Jensen, Wang and de Jong, 2001). The Age-Related Eye Disease Study (AREDS) demonstrated that a dietary supplement containing zinc and antioxidants reduced progression to advanced neovascular AMD (2001). Oxidized proteins lipids and DNA are abundant in eyes with advanced AMD, and proteins with carboxyethylpyrrole (CEP) adducts, derived from the oxidation docosahexanoic acid, are more abundant in the serum and the eyes of AMD patients than in samples from age matched controls (Crabb, Miyagi, Gu, Shadrach, West, Sakaguchi, Kamei, Hasan, Yan, Rayborn, Salomon and Hollyfield, 2002;Hollyfield, Bonilha, Rayborn, Yang, Shadrach, Lu, Ufret, Salomon and Perez, 2008). In RPE of late stage AMD patients, the levels of antioxidant enzymes are elevated, suggesting a defensive response to increased oxidative stress (Decanini, Nordgaard, Feng, Ferrington and Olsen, 2007).

In animal models too, increased oxidative stress to the retina and RPE leads to pathology similar in to AMD in humans, including death of RPE cells and associated photoreceptors. Mice deleted for the *Sod1* gene, encoding CuZn superoxide dismutase, display drusen-like deposits and choroidal neovascularization late in life (Imamura, Noda, Hashizume, Shinoda, Yamaguchi, Uchiyama, Shimizu, Mizushima, Shirasawa and Tsubota, 2006). Iron is an important source of oxidative stress in the retina, and mice deleted for the iron transporters ceruloplasmin and hephaestin demonstrate hypertrophic RPE and subretinal neovascularization (Hadziahmetovic, Dentchev, Song, Haddad, He, Hahn, Pratico, Wen, Harris, Lambris, Beard and Dunaief, 2008).

Mice deleted for the transcription factor Nrf2, which regulates the production anti-oxidant enzymes, develop RPE atrophy, sub-RPE deposits and spontaneous choroidal neovascularization with age (Zhao, Chen, Wang, Sternberg, Freeman, Grossniklaus and Cai, 2011). We have shown that depletion of mitochondrial superoxide dismutase encoded by *Sod2* in mice leads to several characteristic features of dry AMD including increased formation of CEP adducts, increased accumulation of bisretinoid compounds of RPE lipofuscin and death of RPE and photoreceptors (Justilien, Pang, Renganathan, Zhan, Crabb, Kim, Sparrow, Hauswirth and Lewin, 2007;Mao, Seo, Biswal, Li, Conners, Nandyala, Jones, Le and Lewin, 2014;Seo, Krebs, Mao, Jones, Conners and Lewin, 2012).

The 5-hydroxytrptamine (HT) 1a receptor is a potential target for controlling oxidative stress in the retina and RPE. Activation of this receptor is coupled to survival signaling in both neuronal and non-neuronal cells (Cowen, 2007). The 5-HT1a receptor is expressed in the neural retina and the RPE, and the receptor agonist, AL-8309A prevented both complement deposition and retinal degeneration in rats subjected severe photo-oxidative stress (Collier, Patel, Martin, Dembinska, Hellberg, Krueger, Kapin and Romano, 2011;Collier, Wang, Smith, Martin, Ornberg, Rhoades and Romano, 2011). We tested another 5HT1a receptor agonist 8-hydroxy-2-(di-n-propylamino)-tetralin (8-OH DPAT) in mice in which manganese superoxide dismutase (MnSOD)was depleted in the RPE following adeno associated virus (AAV) delivery of a ribozyme specific for *Sod2* mRNA (Thampi, Rao, Mitter, Cai, Mao, Li,

Seo, Qi, Lewin, Romano and Boulton, 2012). Daily injection of this drug for four months prevented both loss of the electroretinogram (ERG) response and thinning of the outer nuclear layer (ONL) seen in eyes treated with vehicle only. We attributed this protection to a decrease in oxidative stress, because oxidative damage to DNA was decreased in the RPE following drug treatment. Furthermore, in ARPE-19 cells exposed to hydrogen peroxide, treatment with 8-OH-DPAT increased the levels of antioxidants such as glutathione and MnSOD.

Since that time, we have developed a model of retinal degeneration based on genetic deletion of *Sod2* in the RPE using cre-lox technology (Mao, Seo, Biswal, Li, Conners, Nandyala, Jones, Le and Lewin, 2014). While mutations in human *SOD2* have not been reliably implicated in AMD, deleting the mouse gene (*Sod2*) permits acceleration of age-related oxidative stress. These mice develop RPE hypertrophy and accumulation of lipofuscin by four months of age and significant loss of the ERG response, corresponding to the death of photoreceptor cells by six months. We decided to revisit the 5-HT1a agonist in this model, because up-regulation of *Sod2* transcription might have overcome the depletion of mRNA by the ribozyme used in the earlier study. We report now that systemic treatment with 8-OH-DPAT elevates the production of other antioxidant and detoxification proteins in the RPE and does, in fact, lead to protection of the retina, even when *Sod2* is deleted in the RPE.

2. Materials and methods

2.1 Experimental mice

Mice were housed in standard caging in a room with a 12h light: 12 hour dark cycle. *Sod2*$^{flox/flox}$*VMD2-cre* mice were transgenic for P_{VMD2}-*rtTA* and *tetO-*P_{hCMV}*cre* and were homozygous for *Sod2* containing *loxP* sites surrounding exon 3, which encodes the manganese binding site of superoxide dismutase. In these mice, cre recombinase is expressed, and *Sod2* is deleted, only in the RPE and only following treatment with doxycycline (Le, Zheng, Rao, Zheng, Anderson, Esumi, Zack and Zhu, 2008). Expression of cre was induced in progeny mice by feeding nursing dams for two weeks with rodent diet containing doxycycline (200 mg/kg; Harlan Rodent dietT-7012, 200 Doxycycline) after birth of the litter (Mao, Seo, Biswal, Li, Conners, Nandyala, Jones, Le and Lewin, 2014).

For four months, *Sod2*$^{flox/flox}$*VMD2-cre* mice were treated by daily subcutaneous injection of 8-OH DPAT at a low (0.5mg/kg) and high dose (5mg/kg) or sterile saline, which was the diluent. At the outset, there were 20 mice per group. In addition, we treated a group of six C57Bl/6J mice with the same treatment regimens for four days, sacrificing mice two hours after the final dose, in order to measure transcript levels for antioxidant enzymes in the retina. For certain procedures, such as electoretinography (ERG), spectral domain optical coherence tomography (SD-OCT) and fundus imaging, mice were anesthetized with a mixture of ketamine (95mg/kg) and xylazine (5-10 mg/kg) by intraperitoneal injection. Local anesthesia for the cornea was provided by 1 drop of proparacaine (1%). At the end of experiments, mice were euthanized either by inhalation of carbon dioxide (>90%) or by injection of 150 mg/kg of sodium pentobarbital (as Euthasol™).

All animal procedures were approved by the University of Florida Institutional Animal Care and Use Committee and were conducted in accordance with the Association for Research in Vision and Ophthalmology (ARVO) Statement for the Use of Animals in Ophthalmic and Vision Research.

2.2 Electroretinography

ERG analysis was performed at the same time of day for each time point, approximately 3 hours after the lights went on in the housing room. Mice were dark-adapted overnight, anesthetized as indicated above, and in dim red light a 2.5% phenylephrine solution was applied to their corneas in order to achieve mydriasis. Gold wire loop contact lenses were placed on each cornea using a drop of CVS brand lubricant solution (0.25% carboxymethylcellulose, 0.3% hypromellose) to maintain corneal hydration. A ground electrode was placed subcutaneously in a hind leg, and a silver wire reference electrode was placed subcutaneously between the eyes. Responses were recorded from both eyes using an LKC UTAS Visual Electrodiagnostic System with a BigShot™ full-field dome (LKC, Gaithersburg, MD). Scotopic ERGs were elicited with 10 msec flashes of white light at 0 dB (2.68 cds/m^2), -10 dB (0.18 cds/m^2), -20 dB (0.02 cds/m^2) with appropriate delay between flashes. Five to 10 scans were averaged at each light intensity.

This was followed by a two minute white light bleach in room light then a white flash at 1.0 cd sec/m^2 intensity was used to elicit a cone response. The a-wave amplitudes were measured from baseline to the peak in the cornea-negative direction, and b-wave amplitudes were measured from cornea-negative peak to major cornea-positive peak. Both a-wave and b-wave amplitudes were measured monthly.

2.3. Spectral domain optical coherence tomography (SD-OCT)

Spectral domain optical coherence tomography (SD-OCT) employed an Envisu ultra high resolution instrument (Bioptigen, Research Triangle Park, NC) at monthly intervals. Mice were dilated and anesthetized as described above for ERG analysis. We collected 300 linear B-scans and 30 images were averaged to minimize the background noise and to achieve a better resolution. Four measurements equidistant from the optical nerve head were recorded from each eye and were analyzed to determine the difference in ONL thickness. The results from each eye were averaged and the means were compared between time points.

2.4. Immunohistochemistry in RPE flat mounts

Mice were euthanized by inhalation with CO_2 and eyes were enucleated. After puncturing the cornea using a 18 gauge needle, the eyes were fixed with 4% paraformaldehyde for 30 minutes at room temperature. The whole eye was then transferred to phosphate buffered saline (PBS). The cornea, lens and neural retina were removed to dissect out eyecups. For antibody staining, eyecups were then rinsed in PBS and pre-incubated in 10% normal goat serum for 1 hour. The eyecups were incubated overnight in rabbit polyclonal anti-8-OHdG antibody at 1:100 (Santa Cruz Biotechnology). After washing four times with wash buffer (0.1% Triton X100 in PBS), the eye cups were incubated in Alexa Fluor 488 phalloidin (Life Technologies) (1:500) and fluorophore-conjugated secondary antibody at 1:500 (Life Technologies) for one hour. After rinsing in PBS, four radial cuts were made and the

eyecups were flattened and mounted on glass slides in Vectashield mounting medium with 4,6-diamino-2-phenylindole (DAPI; Vectashield;Vector Laboratories, Burlingame, CA). The images were taken with a Keyence confocal microscope.

2.5. RNA extraction and qPCR

ARPE-19 cells (ATCC, CRL-2302) were seeded in a 12 well plate at 70% confluence. The next day, the medium was changed to DMEM/F-12 containing 1% FBS. Cells were treated with 300 μM paraquat, 20 μM 8-OH-DPAT, or a combination of the two for the times indicated. Cells were then washed with PBS and total RNA was extracted using the RNeasy Mini Kit from QIAGEN, following the manufacturer's instructions. One microgram of RNA was used to synthesize first strand cDNA using the iScript cDNA synthesis kit from Bio-Rad (Hercules, CA). PCR primers, as shown in Table 1 were synthesized by IDT (Coralville, Iowa). The PCR reaction mixture contained cDNA template, SsoFastEvaGreen Super mix containing SYBR green (Bio-Rad (Hercules, CA), and 3 μM gene specific primers. After denaturation at 95° C for 2 min, 40 cycles of reaction including denaturation at 94° C for 15 sec followed by annealing at 60° C for 30 sec were carried out using C1000 thermal cycler CFX96 real-time system (Bio-Rad). Gene expression was normalized to beta actin. Relative gene expression was compared with untreated samples and determined using the CFX96 software from Bio-Rad.

Mice (C57BL/6, n=5, 8 -10 week old) were treated with 5 mg/kg of 8-OH-DPAT, s.c., for 4 days. Mice were euthanized by CO_2 inhalation and eyes were harvested and dissected to extract the retina. RNA was extracted from the dissociated retinas using the RNeasy Mini Kit from QIAGEN, and the cDNA synthesis and qPCR were carried out as described in the previous paragraph for ARPE-19 cells. The posterior eye cup was dipped in PBS to remove any adherent debris. It was then transferred to a tube containing 200 μl of RNAprotect cell reagent (QIAGEN) and incubated for 10 min at room temperature. The tube was agitated to release RPE cells, as described in (Xin-Zhao Wang, Zhang, Aredo, Lu and Ufret-Vincenty, 2012). The eye cup was removed. RPE cells were centrifuged at 2,500 rpm (680×g) for 5 min. RNA was extracted from the RPE cells as described for the retinas.

2.6. ELISA

Nitrotyrosine levels were estimated using competitive enzyme immunoassay using the Nitrotyrosine Assay Kit, Chemiluminescence Detection from Chemicon International according to the instructions provided in the kit. The RPE/choroid was dissected from four *Sod2*$^{flox/flox}$*VMD2-Cre* mice of each treatment group at two months of age (one month of treatment). The left and right RPE/choroid from each mouse were pooled and sonicated for 10 seconds in Tris-HCl buffered saline, pH7.4, supplied with the kit. Duplicates of each mouse sample and duplicates of each test standard were used in the assay.

2.7. Immunohistochemistry in cells

ARPE-19 cells were grown in eight well chambered slides in a medium containing 1% FBS for 5 weeks until they acquired cuboidal shape. They were treated with 300 μM paraquat, 20 μM 8-OH-DPAT, a combination of the two, or left untreated for another 48 hrs. Cells were fixed with 4% formaldehyde for 30 min at room temperature and washed with PBS,

followed by permeabilization using 1% Triton X-100 in PBS for 30 min at room temperature. Cells were then blocked in 10% normal goat serum in PBS containing 0.5% Triton X-100 for 30 min at room temperature followed by washing in 0.2% Triton X-100 in PBS (wash buffer). Rabbit polyclonal antibody to ZO-1 (Invitrogen) (1:200 dilution) was added and incubated overnight at 4° C, followed by washing. Cy-3 conjugated anti-rabbit secondary antibody (Invitrogen) (1:300 dilution) was added and incubated for 30 min at room temperature, followed by washing. After the addition of mounting media, cells were covered with a cover slip and viewed under a Keyence BZ-X700 fluorescence microscope.

2.8. Transepithelial electrical resistance

ARPE19 cells were plated on 24-well transwell inserts (Greiner-Bio-one, surface area 33.6 mm^2, 0.4 μm pore size) in DMEM/F-12 with 1% FBS for 4 weeks. Paraquat, and/or 8-OH-DPAT was added and incubated for 48 hrs. Transepithelial electrical resistance was measured using an EVOM2 voltohmmeter (World Precision Instruments, Sarasota, FL), according to the manufacturer's instructions. The plates containing the transwells were allowed to equilibrate to room temperature. The inserts were removed one at a time and placed into the EVOM2 chamber filled with DMEM/F-12 basal media. Net TEER measurements were calculated by subtracting the value of a blank transwell filter from the value of each filter with plated cells.

2.9. Histology

Following an overdose of sodium pentobarbital, mice were perfused with 2.5% glutaraldehyde and 2% paraformaldehyde in phosphate buffered saline. Eyes were removed and fixed overnight in freshly prepared 4% paraformaldehyde, 2% glutaraldehyde at 4°C. The tissue was then washed with 0.1M cacodylate buffer (pH7.4) for 10 minutes and incubated in 1% osmium for 4 hours at 4°C. Following osmium treatment, the eyes were incubated in 0.1M cacodylate buffer overnight at 4°C. The tissue was subsequently dehydrated with in a graded series of ethanol concentrations and rotated in epoxy/propylene for embedding. For electron microscopy, sections of 80-100 nm were prepared. Sections of 1μm were made to evaluate the thickness of RPE at each of 10 evenly spaced locations (400μm distance, beginning from optic nerve head) at 5 inferior loci and 5 superior loci along a vertical meridian. Data were collected from 10 readings at each locus with 3 random samplings of the slides from each eye.

2.10. Statistical Analysis

For comparison of the mean amplitudes of multiple groups (e.g., changes in ERG amplitude over time and ONL thickness), we employed one-way analysis of variance (ANOVA) with Tukey's post hoc test. For comparison of mean transcript levels to untreated samples, we used Student's t-test for unpaired samples. In this case, samples were not compared with each other but only to the control (saline) sample for each group.

3. Results

3.1. A 5HT1a Agonist Protects RPE Cells from Mitochondrial Oxidative Stress

Thampi *et al.* reported earlier that treating ARPE-19 cells with 8-OH-DPAT protected them from injury by hydrogen peroxide (Thampi, Rao, Mitter, Cai, Mao, Li, Seo, Qi, Lewin, Romano and Boulton, 2012). We now wanted to determine if this 5-HT1a agonist could protect ARPE-19 cells from reactive oxygen species generated internally, by the mitochondrial electron transport chain. For this purpose, we treated ARPE-19 cells with paraquat, which causes an increase in reactive oxygen species (superoxide and hydrogen peroxide) within mitochondria, largely by interaction with Complex 1 of the respiratory chain (Castello, Drechsel and Patel, 2007;Cocheme and Murphy, 2008). ARPE-19 cells were grown to 70% confluence in low serum medium and exposed to 300 μM paraquat for 24 hours. We observed a dose-dependent impact of 8-OH-DPAT on cell survival: while only 10 % of cells were viable in the absence of 8-OH-DPAT, addition of 3 μM 8-OH-DPAT increased viability to 30% and addition of 30 μM of the 5HT1a agonist led to 65% viability (Fig. 1). Increased survival could also be documented by microscopy: Freshly plated monolayers treated with 300 μM paraquat exhibited gaping holes and cells lifting out of the plane; whereas the monolayer was preserved in cells treated with 8-OH-DPAT plus paraquat (or with DPAT alone) (Fig. 2A-D). If the cells were permitted to grow in 1% FBS containing medium for five weeks, immunofluorescence, using primary antibody to the tight junction protein zona occludens1 (ZO-1), revealed that tight junctions in naïve cells (Fig. 2E) and cells treated with 8-OH-DPAT alone (Fig. 2H) but tight junctions were also apparent in cells treated with paraquat (Fig. 2F) or with 8-OH-DPAT plus paraquat (Fig. 2G). These results suggest that differentiated ARPE-19 cells are resistant to oxidative stress, as documented by the previous work of others (Bailey, Kanuga, Romero, Greenwood, Luthert and Cheetham, 2004;Hsiung, Zhu and Hinton, 2015).

3.2. Induction of Antioxidant Genes by 8-OH-DPAT

Thampi and co-workers (*op. cit.*) had observed an increase in manganese superoxide dismutase (MnSOD) in cells treated with H_2O_2 plus 8-OH-DPAT, and we used quantitative realtime PCR to determine if 8-OH-DPAT plus paraquat had a similar effect (Fig. 3A). Indeed, while treatment with 8-OH-DPAT alone led to a 2.4 fold increase in the level of *SOD2* mRNA in ARPE-19 cells ($p<0.05$), treatment with paraquat and 8-OH-DPAT together caused an 11-fold increase in *SOD2* expression ($p<0.001$), whereas treatment with paraquat alone produced a small decrease in *SOD2* expression. Furthermore, treatment with 8-OH-DPAT in the presence of paraquat led to significant increases in the levels transcripts of five other protective proteins, metallothionein 1 (MT1), heme oxygenase 1 (HO1), NAD(P)H dehydrogenase quinone 1 (NqO1), catalase (Cat) and superoxide dismutase 1 (SOD1). Zinc cations have been shown to protect RPE cells in culture by activation of metallothionein (Tate, Jr., Miceli and Newsome, 1999), and 8-OH-DPAT increases metallothionein production in primary cultured astrocytes (Miyazaki, Asanuma, Murakami, Takeshima, Torigoe, Kitamura and Miyoshi, 2013) suggesting that the drug may protect RPE cells by induction of MT1. HO1 and NqO1 are antioxidant enzymes regulated by transcription factor Nrf2 binding to the antioxidant response elements in their promoters (Calkins, Johnson, Townsend, Vargas, Dowell, Williamson, Kraft, Lee, Li and Johnson,

2008). One might expect, therefore, that they would be up-regulated by paraquat alone. Yet we observed statistically significant increases in HO1 and NqO1 by 8-OH-DPAT that were not further increased by treatment with paraquat.

Differentiated RPE cells that form a characteristic cobblestone appearance with tight junctions are more resistant to oxidative stress than freshly grown RPE cells in culture (Bailey, Kanuga, Romero, Greenwood, Luthert and Cheetham, 2004;Hsiung, Zhu and Hinton, 2015). To determine if drug-treatment affected the sensitivity of these cells to paraquat, we repeated the 8-OH-DPAT treatment, this time using cells that had been grown as monolayers in low serum medium for different intervals up to 30 days. Four days after plating, cells exhibited a low transepithelial resistance (TER) that was completely sensitive to paraquat, though simultaneous treatment with 8-OH-DPAT preserved the TER (Fig. 3B). A similar result was obtained 11 days after plating, but by 18 days, RPE monolayers were resistant to paraquat, and by 30 days cells exhibited a value for TER that was similar to that reported in the literature (Ablonczy, Dahrouj, Tang, Liu, Sambamurti, Marmorstein and Crosson, 2011), and these cells were also resistant to paraquat treatment. When differentiated RPE cells were treated with paraquat and 8-OH-DPAT (Fig. 3C), we observed a 45-fold increase in *MT-1* mRNA and a 22-fold increase in *HO-1* mRNA. The induction of *MT-1* mRNA by 8-OH-DPAT alone was only 2-fold in this experiment, and the increase *MT-1* expression with paraquat alone was 27-fold., showing that the combined effect was roughly the product of the individual treatments. There was a small increase (less than 2-fold) in the expression of catalase following paraquat treatment, but using differentiated ARPE-19 monolayers there was *no* induction of *SOD1* expression *or SOD2* expression in cells treated with either compound or with the combination of paraquat plus 8-OH-DPAT.

3.3. 8-OH-DPAT Stimulates Antioxidant Gene Expression in the Retina

Because differentiated RPE cells responded to 8-OH-DPAT and to mitochondrial oxidative stress differently than did freshly grown ARPE-19 cells, we decided to test the impact of the drug on the same marker genes in mice. Mice were treated on four sequential days with subcutaneous injections of 5 mg/kg of 8-OH-DPAT or of sterile saline. Based on body surface area, this dose would correspond to 0.4 mg/kg in an adult (60 kg) human (Reagan-Shaw, Nihal and Ahmad, 2008). We then analyzed the dissected neural retinas and the RPE for measurement of transcript levels using RT-PCR (Fig. 4). In the retina (Fig. 4A), the 5HT1a agonist resulted in a 2- fold increase in the expression of *MT-1* ($p<0.001$), a 4-fold increase in *HO-1* ($p<0.01$), a 1.7 fold increase in both *NqO1* and catalase ($p<0.05$), and a 1.6 fold increase in SOD1 ($p<0.01$). However, there was no induction of SOD2. This result suggests that any anti-oxidant protection we may observe is not associated with increased production of MnSOD, but rather with other protective proteins such as metallothionein and antioxidant enzymes, such heme oxygenase 1, NAD(P)H-dehydrogenase quinone 1, catalase and Cu/Zn superoxide dismutase.

Similar to what we observed in differentiated ARPE-19 cells, treatment of mice with 8-OH-DPAT alone, led to only a marginal increase in the expression of MT1 and HO-1, and no statistically significant change in NqO1 and SOD2 in the RPE (Fig. 4B). If anything, the

levels of catalase and SOD1 mRNA were slightly decreased in the RPE of mice treated with 8-OH-DPAT.

3.4. Reduced oxidative stress in RPE-Specific Sod2 knockout mice

We next asked if 8-OH-DPAT treatment could attenuate oxidative stress we reported in mice deleted for the *Sod2* gene in the RPE. These mice are homozygous for a floxed (flanked by loxP) allele of *Sod2* (Strassburger, Bloch, Sulyok, Schuller, Keist, Schmidt, Wenk, Peters, Wlaschek, Lenart, Krieg, Hafner, Kumin, Werner, Muller and Scharffetter-Kochanek, 2005) and bear a doxycycline-regulated copy of the cre recombinase that is expressed only in the RPE, because the tetracycline transactivator is expressed under control of the *VMD2* promoter (Le, Zheng, Rao, Zheng, Anderson, Esumi, Zack and Zhu, 2008). We had previously reported an increase in the level of 8-OH-deoxyguanosine in the RPE layer of these mice that was evident by immunohistochemistry in RPE flat mounts (Mao, Seo, Biswal, Li, Conners, Nandyala, Jones, Le and Lewin, 2014). To determine if 8-OH-DPAT treatment reduced oxidative stress in these mice, we induced neonatal mice for expression of cre recombinase, and at one month of age, in different groups of mice we began daily subcutaneous injection of sterile saline, 0.5 mg/kg or 5.0 mg/kg of 8-OH-DPAT dissolved in sterile saline. After 30 days of treatment, 3 mice from each group were humanely sacrificed, and RPE flat mounts were prepared. While considerable immunofluorescence was apparent in the mice treated with saline or with the lose dose of 8-OH-DPAT, treatment with 5.0 mg/kg reduced the level of 8-OH-deoxyguanosine immune reactivity substantially (Fig. 5A-C).

To test another marker of oxidative stress in *Sod2* deleted mice treated with 8-OH-DPAT, proteins were extracted from four mice from each treatment group and assayed for nitrotyrosine by ELISA. Reaction of superoxide with nitric oxide results in peroxynitrite ($ONOO^-$), and nitrotyrosine adducts are formed by reaction of peroxynitrate with tyrosine residues. We observed a six-fold reduction in nitrotyrosine adducts in the RPE samples of mice treated with either the low-dose or the high dose of 8-OH-DPAT (Fig. 6A). Overall, levels of nitrotyrosine were lower in the neural retina, but treatment with 5 mg/kg of 8-OH-DPAT led to a three-fold reduction in nitrotyrosine, (Fig. 6B) ($p=0.058$).

3.5. Protection of Visual Function by Daily Treatment with 5HT1a Agonist

To determine if reducing oxidative stress in the retina and RPE would preserve photoreceptor function in mice deleted for *Sod2* in the RPE, we gave *Sod2*$^{flox/flox}$ *VMD2-cre* mice that had been induced with doxycycline as neonates, daily injections of 8-OH-DPAT at a low (0.5 mg/kg) or a high dose (5.0 mg/kg), while a control group was given daily injections of diluent (sterile saline) over a period of four months. To assess visual function we performed dark-adapted full field electoretinography (ERG) measurements at monthly intervals (Fig. 7). While daily treatment with the low dose of did not affect the a-wave or b-wave amplitudes in *Sod2* deleted mice, treatment with the higher dose led to a 50% increase in amplitudes of a-wave and b-wave that was maintained over the four-month time course. There was no significant difference between the implicit time (latency) of the a-wave and the b-wave among the mice in the three treatment groups. Cone function as measured by

photopic b-wave amplitudes did not decline significantly over the four-month time course, and consequently we saw no impact of drug treatment (data not shown).

To determine if drug treatment had an impact on functional vision, we performed an optokinetic assessment (Optomotry™) following four months of treatment (Fig. 8). We observed that daily injection of either 0.5 mg/kg or 5.0 mg/kg of drug led to a modest (20%) but statistically significant increase in visual acuity, measured as cycles per degree. Because visual acuity can be improved by localized preservation of retinal function, it is not unexpected that optokinetic assessment should be more sensitive than full field ERG, perhaps accounting for the difference in results between ERG and Optomotry™ at the low drug level.

3.6. Impact of 8-OH-DPAT Treatment on Retinal and RPE Structure

To assess impact of drug treatment on retinal structure, we used spectral domain optical coherence tomography (SD-OCT) to evaluate the thickness of the outer nuclear layer (ONL) measuring at four locations equidistant from the optic nerve head and averaging these measurements (Fig. 9). We observed a slight, but statistically insignificant, reduction in the ONL thickness over the course of the experiment, and, if anything, high dose 8-OH-DPAT treatment led to a marginal decrease in ONL thickness, though this difference did not attain statistical significance either. Nevertheless, SD-OCT did reveal important differences between treatment groups with respect to outer rod-outer segments (Fig. 10A). In human eyes, Staurenghi *et al.* (Staurenghi, Sadda, Chakravarthy and Spaide, 2014) have identified the photoreceptor outer segments as a hypo-reflective band above the RPE choroid complex. Recent work using signal-averaged images and experimental manipulation in mice (Berger, Cavallero, Dominguez, Barbe, Simonutti, Sahel, Sennlaub, Raoul, Paques and Bemelmans, 2014) corroborates that assignment. We consistently observed that this layer was noisier and more hyper-reflective in the *Sod2* deleted mice treated only with saline than in mice treated with the high dose of 8-OH-DPAT. Mice treated with a low dose of the drug exhibited intermediate reflectivity of this layer.

Electron micrographs from the same mice indicate a potential source of increased reflectance: In saline treated animals (Control) the outer segments were disordered and contained holes or cystic spaces within the outer segments (Fig. 10B). Photoreceptors in mice treated with 0.5 mg/ml of 8-OH-DPAT were also disordered, and, as in the saline treated mice, they exhibited broken tips that had not been phagocytized by the RPE. In contrast, photoreceptors in mice treated with the high dose of 8-OH-DPAT exhibited uniform thickness and regularly arranged disc membranes. The tips of the outer segments of the photoreceptors did not appear to interdigitate with apical processes of the RPE, however.

It was obvious that the RPE of the control treated mice were more highly vacuolated than that of the high dose group (Fig. 11A and B). RPE vacuolization was widespread, as demonstrated by light micrographs taken at lower magnification (Supplementary Fig. 1). Light micrographs like these were used to measure the thickness of the RPE layer at ten evenly spaced locations along a vertical meridian containing the optic nerve head. No significant differences in RPE thickness were found between the control and high dose groups, though the RPE was measurably thicker at several locations in mice treated with the

low dose of 8-OH-DPAT (Supplementary Fig. 2). We currently have no explanation for this finding. More mitochondria were visible in the 8-OH-DPAT treated mice, and most of these were along the basal surface (Fig. 11B). In the saline treated mice, melanosomes were located primarily along the apical surface but they were more spherical than the typical elongated melanosomes seen in the drug treated mice. The in-foldings along the basal surface of the RPE appeared mode densely packed in the high dose-treated eyes, and Bruch's membrane retained a more compact structure in mice of this group. These are characteristics of the RPE in wild-type mice. Mice treated with the low dose of 8-OH-DPAT exhibited damaged outer segments and an intermediate level of vacuolization compared to the other groups (Supplementary Fig. 3), but alterations to Bruch's membrane and to the basal surface of the RPE were less severe changes seen in the control (saline treated) mice.

4. Discussion

Serotonin receptor agonists and antagonists are commonly used to treat depression or anxiety, and a 5HT1a receptor agonist, Buspirone, is currently in use for that purpose. However, 5HT1a receptor agonists also have neuroprotective effects (Ramos, Rubio, Defagot, Hischberg, Villar and Brusco, 2004), and one orally available agonist, xaliproden, has been shown to reduce neuropathic side-effects of chemotherapy (Susman, 2006). This drug has also been used in clinical trials for ALS and Alzheimer disease. Another 5HT1a agonist, AL-78898A, has been employed as localized treatment for patients with geographic atrophy associated with AMD (www.clinicaltrials.gov). While efficacy has yet to be established in any of the clinical trials, the drugs appear to be safe, and we believe that continuing to explore the benefit of 5HT1a receptor agonists as a treatment for geographic atrophy is warranted, especially in light of the protective effect of these compounds in rodent models of retinal injury (Collier, Patel, Martin, Dembinska, Hellberg, Krueger, Kapin and Romano, 2011;Collier, Wang, Smith, Martin, Ornberg, Rhoades and Romano, 2011;Thampi, Rao, Mitter, Cai, Mao, Li, Seo, Qi, Lewin, Romano and Boulton, 2012). We have used the prototype compound of this class, 8-OH-DPAT, in a mouse model of geographic atrophy associated with mitochondrial reactive oxygen species in the RPE.

We show that in the face of mitochondrial oxidative stress, treating ARPE-19 cells with this agonist led to a significant increase in the expression anti-oxidant enzymes such as HO-1, NqO1, Cu/Zn SOD (SOD1) and catalase which are regulated by transcription factor Nrf2, and of MnSOD, which is regulated independently (Fig. 3). In addition, transcript levels of the metallothionein were increased by simultaneous treatment with 8-OH-DPAT and paraquat. Zinc treatment of ARPE 19 cells was also shown to stimulate this production of this metal binding protein, resulting in lysosomal stabilization and protection from oxidative stress (Baird, Kurz and Brunk, 2006). Karlsson *et al.* (Karlsson, Frennesson, Gustafsson, Brunk, Nilsson and Kurz, 2013) suggest that autophagy of iron binding proteins such as metallothionein protects the RPE by reducing the level of reactive iron in the lysosome. As expected, elevation of these proteins protected cultured RPE cells from cell death (Fig. 1) and preserved the integrity of RPE monolayers (Fig. 2 and Fig. 3B).

Strikingly, when RPE cells were grown for several weeks in low serum medium to stimulate differentiation into a monolayer of cells that exhibited trans-epithelial resistance, *Sod2*

expression was not stimulated by 8-OH-DPAT. Differentiated RPE cells are known to be resistant to treatment with oxidants, and the basal levels molecular chaperons is already elevated under these conditions (Bailey, Kanuga, Romero, Greenwood, Luthert and Cheetham, 2004). We noticed that the induction of metallothionein and heme oxygenaseidase 1 were much higher in differentiated ARPE-19 monolayers than in freshly grown cells (Fig. 3C).

Systemic treatment of mice for four days with 8-OH-DPAT stimulated transcription of metallothionein and Nrf2 regulated anti-oxidant genes in the neural retina, but not *Sod2*. The level of induction of metallothionein and heme oxygenase 1 was much lower in the RPE following drug treatment, but was similar to the level of induction seen in differentiated RPE cells treated with 8-HO-DPAT. In the differentiated RPE cells, high level induction required both drug treatment and mitochondrial oxidative stress (paraquat). In mice deleted for *Sod2* in the RPE, treatment with the 5HT1a agonist led to a decrease in RPE oxidative stress, as measured by immune reactivity of 8-OH-deoxyguanosine in the RPE (Fig. 5) and reduction in nitrotyrosine adducts (Fig. 6). We conclude that 8-OH-DPAT protects the RPE and neural retina by elevation of antioxidant proteins other than MnSOD, and the protection we had observed in the ribozyme-knockdown model (Thampi, Rao, Mitter, Cai, Mao, Li, Seo, Qi, Lewin, Romano and Boulton, 2012) was not a simple reversal of the original injury.

To confirm this conclusion, we initiated a long term (four month) study of systemic drug therapy in mice deleted for *Sod2* in the RPE. In this case, since the gene was missing, levels of *Sod2* mRNA in the RPE could not be elevated in response to 8-OH-DPAT, and we confirmed this by RT-PCR (data not shown). We did not expect to measure significant changes in ERG amplitudes in response to drug treatment, since reduction in ERG amplitudes did not become statistically significant before six months in the *Sod2* deleted mice (Mao, Seo, Biswal, Li, Conners, Nandyala, Jones, Le and Lewin, 2014). We did, nevertheless, observe a statistically significant increase in ERG a-wave and b-wave amplitudes in $Sod2^{flox/flox}$*VMD2-cre* mice treated with 5.0 mg/kg of 8-OH-DPAT (Fig. 7). This elevation in electroretinogram response was not seen in wild-type (C57Bl/6) mice in response to daily high dose treatment (Thampi, Rao, Mitter, Cai, Mao, Li, Seo, Qi, Lewin, Romano and Boulton, 2012). Therefore, we conclude that the protective effect measured by ERG was related to the elevation in protective proteins (Fig. 3 & 4) and the reduction in oxidative stress (Fig. 5) in high-dose treated mice relative to control or low dose groups.

The most striking impact of treatment with 8-OH-DPAT was revealed by electron microscopy. Doxycycline induced $Sod2^{flox/flox}$*VMD2-cre* mice, exhibited vacuolization of the RPE that was not observed in mice treated with the high dose of the drug (Figs. 10 & 11). In addition, drug therapy preserved the structure of the rod photoreceptor outer segments, which contained distorted disc membranes and broken tips in mice treated with saline or with the low dose of 8-OH-DPAT. Consequently, it is likely that the phagocytic function of RPE was compromised by mitochondrial oxidative stress, and that drug treatment protected this essential function. In future work, we plan to use primary cell cultures from the RPE of affected and treated mice to test this hypothesis using a phagocytosis assay (Nandrot, Kim, Brodie, Huang, Sheppard and Finnemann, 2004).

A finding that we cannot explain at this time is that treatment with both low dose and high dose of 8-OH-DPAT led to reduced oxidative stress in the RPE and that both dosing levels improved the optokinetic response (Fig. 8), but that only daily dosing with 5.0 mg/kg (the high dose) seemed to preserve the structure of the photoreceptors. The 5HT1a receptor is a G protein coupled receptor that mediates a variety of responses depending on the cell type (Kushwaha and Albert, 2005;Liu and Albert, 1991;Wang, Terauchi, Yee, Umemori and Traynor, 2014). For example, in serotonergic neurons, the receptor inhibits adenylate cyclase activity leading to inhibition of N-type calcium channels, and reducing neuronal activity. In contrast, in fibroblasts activation of this receptor stimulates phospholipase C activity and leads to an influx of Ca^{+2} and protein kinase C activation. In addition, 8-OH-DPAT binding to the 5HT1a receptor activates the MAPK (mitogen activated protein kinase) in fibroblast cells (Garnovskaya, van, Hawe, Casanas, Lefkowitz and Raymond, 1996). Treatment with the high dose of 8-OH-DPAT may have had multiple effects on the retina and RPE, in addition to increasing protection from mitochondrial oxidative stress. This multiplicity of effects suggests that studying the mechanism of action of this class of compounds in the retina could be fruitful for understanding basic signaling processes as well as for therapy.

Conclusions

8-OH-DPAT was effective in preserving RPE structure and function and in preventing the loss of photoreceptors in this this model of retinal degeneration and in the more severe light injury model. Whether systemic delivery of 5HT1a agonists will be useful for treating dry AMD and preventing atrophy of the RPE may depend on the tolerability of their side effects. The compounds that are already approved for human use have mood altering properties, and these may limit the usefulness of these drugs for long-term use. On the other hand, if a selective agonist can be identified or a method for localized delivery to the back of the eye can be developed (Cholkar, Gunda, Earla, Pal and Mitra, 2014;Rowe-Rendleman, Durazo, Kompella, Rittenhouse, Di, Weiner, Grossniklaus, Naash, Lewin, Horsager and Edelhauser, 2014), then 5HT1a agonists have great promise for the treatment of advanced AMD.

Supplementary Material

Refer to Web version on PubMed Central for supplementary material.

Acknowledgments

This work was supported by grants from the BrightFocus Foundation and from Alcon Laboratories, Inc. Additional support was provided by the Shaler Richardson Professorship endowment and by the NEI core grant to the University of Florida (P30 EY02172). We thank Dr. Eduardo Candelario-Jalil for allowing us to use his voltohmmeter to measure transepithelial resistance and to Dr. Changjun Yang for teaching us how to use it.

References

1. A randomized, placebo-controlled, clinical trial of high-dose supplementation with vitamins C and E and beta carotene for age-related cataract and vision loss: AREDS report no. 9. Arch Ophthalmol. 2001; 119:1439–52. [PubMed: 11594943]

2. Ablonczy Z, Dahrouj M, Tang PH, Liu Y, Sambamurti K, Marmorstein AD, Crosson CE. Human Retinal Pigment Epithelium Cells as Functional Models for the RPE In Vivo. Investigative Ophthalmology & Visual Science. 2011; 52:8614–20. [PubMed: 21960553]

3. Bailey TA, Kanuga N, Romero IA, Greenwood J, Luthert PJ, Cheetham ME. Oxidative stress affects the junctional integrity of retinal pigment epithelial cells. Invest Ophthalmol Vis Sci. 2004; 45:675–84. [PubMed: 14744914]

4. Baird SK, Kurz T, Brunk UT. Metallothionein protects against oxidative stress-induced lysosomal destabilization. Biochem J. 2006; 394:275–83. [PubMed: 16236025]

5. Berger A, Cavallero S, Dominguez E, Barbe P, Simonutti M, Sahel JA, Sennlaub F, Raoul W, Paques M, Bemelmans AP. Spectral-domain optical coherence tomography of the rodent eye: highlighting layers of the outer retina using signal averaging and comparison with histology. PLoS ONE. 2014; 9:e96494. [PubMed: 24788712]

6. Calkins MJ, Johnson DA, Townsend JA, Vargas MR, Dowell JA, Williamson TP, Kraft AD, Lee JM, Li J, Johnson JA. The Nrf2/ARE pathway as a potential therapeutic target in neurodegenerative disease. Antioxid Redox Signal. 2008

7. Cano M, Thimmalappula R, Fujihara M, Nagai N, Sporn M, Wang AL, Neufeld AH, Biswal S, Handa JT. Cigarette Smoking, Oxidative stress, the Antioxidant response through Nrf2 signaling, and Age-related Macular Degeneration. Vision Research In Press, Accepted Manuscript.

8. Castello PR, Drechsel DA, Patel M. Mitochondria Are a Major Source of Paraquat-induced Reactive Oxygen Species Production in the Brain. J Biol Chem. 2007; 282:14186–93. [PubMed: 17389593]

9. Cholkar K, Gunda S, Earla R, Pal D, Mitra AK. Nanomicellar Topical Aqueous Drop Formulation of Rapamycin for Back-of-the-Eye Delivery. AAPS PharmSciTech. 2014; 16:610–22. [PubMed: 25425389]

10. Cocheme HM, Murphy MP. Complex I is the major site of mitochondrial superoxide production by paraquat. J Biol Chem. 2008; 283:1786–98. [PubMed: 18039652]

11. Collier RJ, Patel Y, Martin EA, Dembinska O, Hellberg M, Krueger DS, Kapin MA, Romano C. Agonists at the serotonin receptor (5-HT(1A)) protect the retina from severe photo-oxidative stress. Invest Ophthalmol Vis Sci. 2011; 52:2118–26. [PubMed: 21087971]

12. Collier RJ, Wang Y, Smith SS, Martin E, Ornberg R, Rhoades K, Romano C. Complement deposition and microglial activation in the outer retina in light-induced retinopathy: inhibition by a 5-HT1A agonist. Invest Ophthalmol Vis Sci. 2011; 52:8108–16. [PubMed: 21467172]

13. Cowen DS. Serotonin and neuronal growth factors - a convergence of signaling pathways. J Neurochem. 2007; 101:1161–71. [PubMed: 17286594]

14. Crabb JW, Miyagi M, Gu X, Shadrach K, West KA, Sakaguchi H, Kamei M, Hasan A, Yan L, Rayborn ME, Salomon RG, Hollyfield JG. From the Cover: Drusen proteome analysis: An approach to the etiology of age-related macular degeneration. Proceedings of the National Academy of Sciences. 2002; 99:14682–7.

15. Decanini A, Nordgaard CL, Feng X, Ferrington DA, Olsen TW. Changes in select redox proteins of the retinal pigment epithelium in age-related macular degeneration. Am J Ophthalmol. 2007; 143:607–15. [PubMed: 17280640]

16. Garnovskaya MN, van BT, Hawe B, Casanas RS, Lefkowitz RJ, Raymond JR. Ras-dependent activation of fibroblast mitogen-activated protein kinase by 5-HT1A receptor via a G protein beta gamma-subunit-initiated pathway. Biochemistry. 1996; 35:13716–22. [PubMed: 8901512]

17. Hadziahmetovic M, Dentchev T, Song Y, Haddad N, He X, Hahn P, Pratico D, Wen R, Harris ZL, Lambris JD, Beard J, Dunaief JL. Ceruloplasmin/hephaestin knockout mice model morphologic and molecular features of AMD. Invest Ophthalmol Vis Sci. 2008; 49:2728–36. [PubMed: 18326691]

18. Hollyfield JG, Bonilha VL, Rayborn ME, Yang X, Shadrach KG, Lu L, Ufret RL, Salomon RG, Perez VL. Oxidative damage-induced inflammation initiates age-related macular degeneration. Nat Med. 2008; 14:194–8. [PubMed: 18223656]

19. Hsiung J, Zhu D, Hinton DR. Polarized Human Embryonic Stem Cell-Derived Retinal Pigment Epithelial Cell Monolayers Have Higher Resistance to Oxidative Stress-Induced Cell Death Than Nonpolarized Cultures. Stem Cells Translational Medicine. 2015; 4:10–20. [PubMed: 25411476]

20. Imamura Y, Noda S, Hashizume K, Shinoda K, Yamaguchi M, Uchiyama S, Shimizu T, Mizushima Y, Shirasawa T, Tsubota K. Drusen, choroidal neovascularization, and retinal pigment epithelium dysfunction in SOD1-deficient mice: a model of age-related macular degeneration. Proc Natl Acad Sci U S A. 2006; 103:11282–7. [PubMed: 16844785]
21. Jarrett SG, Boulton ME. Consequences of oxidative stress in age-related macular degeneration. Molecular Aspects of Medicine. 2012; 33:399–417. [PubMed: 22510306]
22. Justilien V, Pang JJ, Renganathan K, Zhan X, Crabb JW, Kim SR, Sparrow JR, Hauswirth WW, Lewin AS. SOD2 knockdown mouse model of early AMD. Invest Ophthalmol Vis Sci. 2007; 48:4407–20. [PubMed: 17898259]
23. Karlsson M, Frennesson C, Gustafsson T, Brunk UT, Nilsson SE, Kurz T. Autophagy of iron-binding proteins may contribute to the oxidative stress resistance of ARPE-19 cells. Exp Eye Res. 2013; 116:359–65. [PubMed: 24416768]
24. Kushwaha N, Albert PR. Coupling of 5-HT1A autoreceptors to inhibition of mitogen-activated protein kinase activation via G beta gamma subunit signaling. Eur J Neurosci. 2005; 21:721–32. [PubMed: 15733090]
25. Le YZ, Zheng W, Rao PC, Zheng L, Anderson RE, Esumi N, Zack DJ, Zhu M. Inducible expression of cre recombinase in the retinal pigmented epithelium. Invest Ophthalmol Vis Sci. 2008; 49:1248–53. [PubMed: 18326755]
26. Liu YF, Albert PR. Cell-specific signaling of the 5-HT1A receptor. Modulation by protein kinases C and A. J Biol Chem. 1991; 266:23689–97. [PubMed: 1660881]
27. Mao H, Seo SJ, Biswal MR, Li H, Conners M, Nandyala A, Jones K, Le YZ, Lewin AS. Mitochondrial oxidative stress in the retinal pigment epithelium leads to localized retinal degeneration. Invest Ophthalmol Vis Sci. 2014; 55:4613–27. [PubMed: 24985474]
28. Miyazaki I, Asanuma M, Murakami S, Takeshima M, Torigoe N, Kitamura Y, Miyoshi K. Targeting 5-HT(1A) receptors in astrocytes to protect dopaminergic neurons in Parkinsonian models. Neurobiol Dis. 2013; 59:244–56. [PubMed: 23959140]
29. Nandrot EF, Kim Y, Brodie SE, Huang X, Sheppard D, Finnemann SC. Loss of synchronized retinal phagocytosis and age-related blindness in mice lacking alphavbeta5 integrin. J Exp Med. 2004; 200:1539–45. [PubMed: 15596525]
30. Ramos AJ, Rubio MD, Defagot C, Hischberg L, Villar MJ, Brusco A. The 5HT1A receptor agonist, 8-OH-DPAT, protects neurons and reduces astroglial reaction after ischemic damage caused by cortical devascularization. Brain Res. 2004; 1030:201–20. [PubMed: 15571670]
31. Reagan-Shaw S, Nihal M, Ahmad N. Dose translation from animal to human studies revisited. FASEB J. 2008; 22:659–61. [PubMed: 17942826]
32. Rowe-Rendleman CL, Durazo SA, Kompella UB, Rittenhouse KD, Di PA, Weiner AL, Grossniklaus HE, Naash MI, Lewin AS, Horsager A, Edelhauser HF. Drug and gene delivery to the back of the eye: from bench to bedside. Invest Ophthalmol Vis Sci. 2014; 55:2714–30. [PubMed: 24777644]
33. Seo SJ, Krebs MP, Mao H, Jones K, Conners M, Lewin AS. Pathological consequences of long-term mitochondrial oxidative stress in the mouse retinal pigment epithelium. Exp Eye Res. 2012; 101:60–71. [PubMed: 22687918]
34. Shen JK, Dong A, Hackett SF, Bell WR, Green WR, Campochiaro PA. Oxidative damage in age-related macular degeneration. Histol Histopathol. 2007; 22:1301–8. [PubMed: 17701910]
35. Smith W, Assink J, Klein R, Mitchell P, Klaver CC, Klein BE, Hofman A, Jensen S, Wang JJ, de Jong PT. Risk factors for age-related macular degeneration: Pooled findings from three continents. Ophthalmology. 2001; 108:697–704. [PubMed: 11297486]
36. Staurenghi G, Sadda S, Chakravarthy U, Spaide RF. Proposed lexicon for anatomic landmarks in normal posterior segment spectral-domain optical coherence tomography: the IN*OCT consensus. Ophthalmology. 2014; 121:1572–8. [PubMed: 24755005]
37. Strassburger M, Bloch W, Sulyok S, Schuller J, Keist AF, Schmidt A, Wenk J, Peters T, Wlaschek M, Lenart J, Krieg T, Hafner M, Kumin A, Werner S, Muller W, Scharffetter-Kochanek K. Heterozygous deficiency of manganese superoxide dismutase results in severe lipid peroxidation and spontaneous apoptosis in murine myocardium in vivo. Free Radic Biol Med. 2005; 38:1458–70. [PubMed: 15890620]

38. Susman E. Xaliproden lessens oxaliplatin-mediated neuropathy. Lancet Oncol. 2006; 7:288. [PubMed: 16598880]

39. Tate DJ Jr, Miceli MV, Newsome DA. Zinc protects against oxidative damage in cultured human retinal pigment epithelial cells. Free Radic Biol Med. 1999; 26:704–13. [PubMed: 10218660]

40. Thampi P, Rao HV, Mitter SK, Cai J, Mao H, Li H, Seo S, Qi X, Lewin AS, Romano C, Boulton ME. The 5HT(1a) Receptor Agonist 8-Oh DPAT Induces Protection from Lipofuscin Accumulation and Oxidative Stress in the Retinal Pigment Epithelium. PLoS ONE. 2012; 7:e34468. [PubMed: 22509307]

41. Wang Q, Terauchi A, Yee CH, Umemori H, Traynor JR. 5-HT1A receptor-mediated phosphorylation of extracellular signal-regulated kinases (ERK1/2) is modulated by regulator of G protein signaling protein 19. Cell Signal. 2014; 26:1846–52. [PubMed: 24793302]

42. Xin-Zhao Wang C, Zhang K, Aredo B, Lu H, Ufret-Vincenty RL. Novel method for the rapid isolation of RPE cells specifically for RNA extraction and analysis. Exp Eye Res. 2012; 102:1–9. [PubMed: 22721721]

43. Zhao Z, Chen Y, Wang J, Sternberg P, Freeman ML, Grossniklaus HE, Cai J. Age-related retinopathy in NRF2-deficient mice. ONE. 2011; 6:e19456.

Highlights

- Oxidative stress contributes to the pathology of age related macular degeneration (AMD).
- Activation of the serotonin 5HT1a receptor stimulates survival pathways.
- A 5HT1a agonist protected RPE cells from mitochondrial oxidative stress.
- The same agonist protected the retina and retinal pigment epithelium in a mouse model with increased oxidative stress in the RPE.
- Stimulation of this pathway may prevent geographic atrophy, the advanced form of dry AMD.

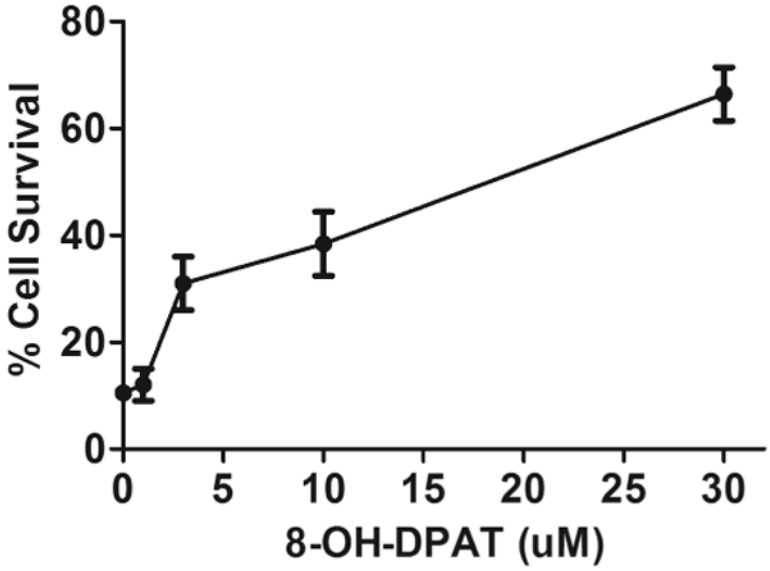

Fig. 1.

8-OH-DPAT prevents RPE cell killing by mitochondrial oxidative stress. ARPE19 cells were seeded at 70% confluence in medium containing with 1% FBS and allowed to grow overnight. Then cells were treated with 300 μM paraquat and increasing amounts of 8-OH-DPAT, as indicated. Two days later, cells were stained with CellTiter Aqueous (Promega) and the absorbance read in a plate reader. Survival of cells was calculated using the absorbance of cells not treated with paraquat as 100%.

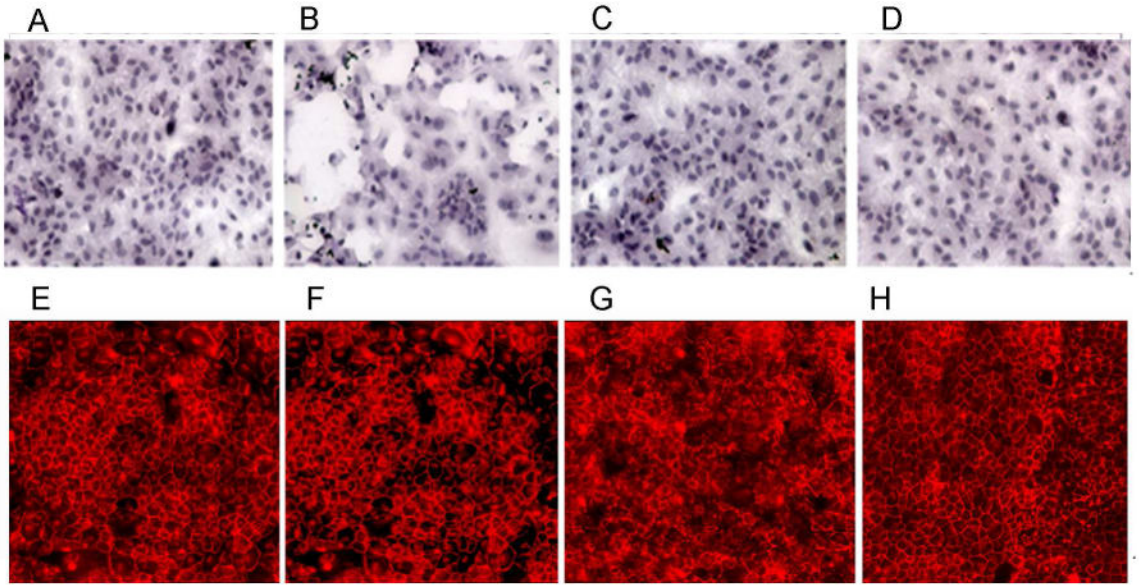

Fig. 2.

8-OH-DPAT protects against the loss of tight junctions caused by mitochondrial oxidative stress. (A-D) ARPE-19 cells were grown overnight in low serum medium. They were then treated with paraquat (300 μM), or 8-OH-DPAT (20 μM), or a combination of the two for 48 hours, or left untreated. Cells were fixed, stained with hematoxylin and eosin, and imaged by light microscopy at an original magnification of 20×. (E-H) ARPE-19 cells were grown for five weeks in low serum medium until a change to cuboidal shape was noticeable. They were then treated with paraquat (300 μM), or 8-OH-DPAT (20 μM), or a combination of the two for 48 hr, or left untreated. Cells were then permeabilized by treatment with non-ionic detergent and incubated with an antibody to ZO-1, followed by treatment with a Cy3 conjugated secondary antibody. Cells were visualized by fluorescence microscopy. A & E: cells in medium only; B & F: 300 μM paraquat; C & G: 300 μM paraquat plus 20 μM 8-OH-DPAT; D & H: 20 μM 8-OH-DPAT only.

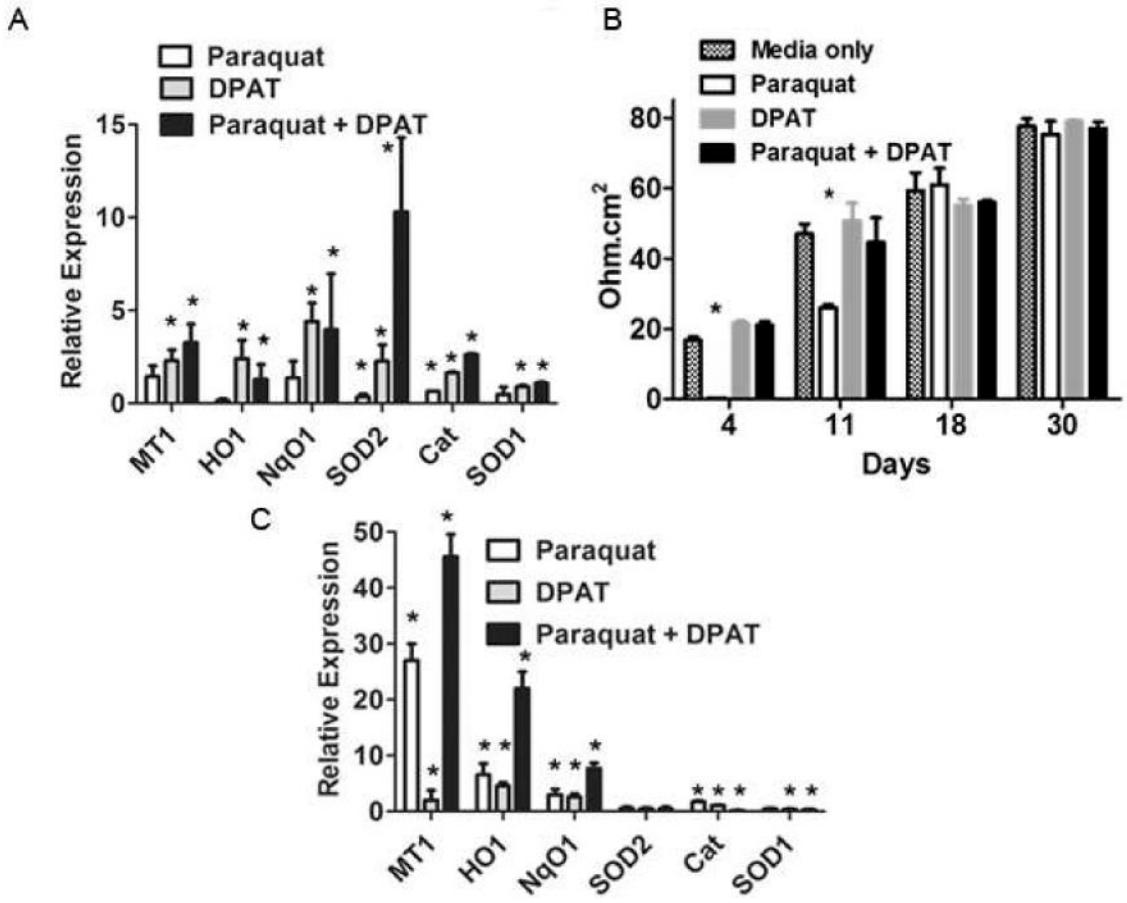

Fig. 3.

8-OH-DPAT enhances the antioxidant response. **A.** ARPE-19 cells were treated simultaneously with 300 μM paraquat and 20 μM 8-OH-DPAT for 48 hrs. RNA was extracted, followed by first strand cDNA synthesis and qPCR with primers for mRNAs encoding the antioxidant effector molecules indicated. Assays were performed in triplicate. Transcript levels relative to beta actin were set to one in untreated cells, and the values indicated are relative to untreated cells (*$p<0.05$ relative to untreated cells) Error bars indicate the standard deviation. **B.** ARPE-19 cells grown in low serum medium for days indicated were treated with paraquat (400 μM), and or 8-OH-DPAT (20 μM) for the last 48 hr. Electrical resistance was measured using EVOM2 (World Precision Instruments). Resistance in no cell control well was subtracted from those with cells (*$p<0.05$ relative to media only) Error bars indicate the standard deviation. **C.** ARPE-19 cells grown in low serum medium for 5 weeks were treated with paraquat, 8-OH-DPAT, or a combination of the two for 48 hrs. RNA was extracted and first strand cDNA was synthesized, which was used to carry out qPCR with the primers for the genes indicated. Transcript levels relative to beta actin were set to one in untreated cells, and the values indicated are relative to untreated cells (*$p<0.05$ relative to untreated cells). Error bars indicate the standard deviation.

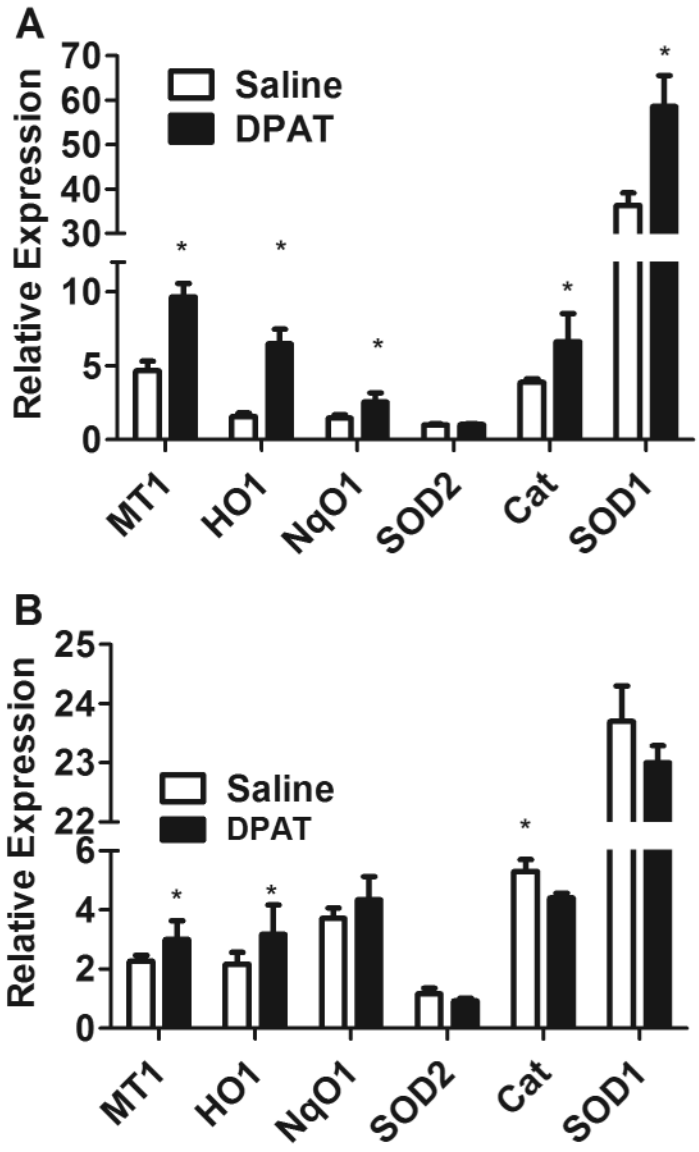

Fig. 4.

The 5HT1a agonist induces antioxidant enzymes in the neural retina. Mice (n=5, 8 to 10 week old) were injected daily subcutaneously with 5 mg/kg of 8-OH-DPAT, or equivalent volume of saline for 4 days. Retina and retinal pigment epithelium, dissected from the eyes of these mice were used to extract RNA, which was used for RT-qPCR to evaluate the expression of metallothionein 1 (MT1), heme oxygenase 1 (HO1), NqO1, or superoxide dismutase 2 (SOD2), catalase (Cat) and superoxide dismutase 1 (SOD1) relative to β-actin (*$p<0.05$ compared to saline). A. Results for the neural retina; B. Results for the RPE. Error bars indicate the standard deviation (*$p<0.05$).

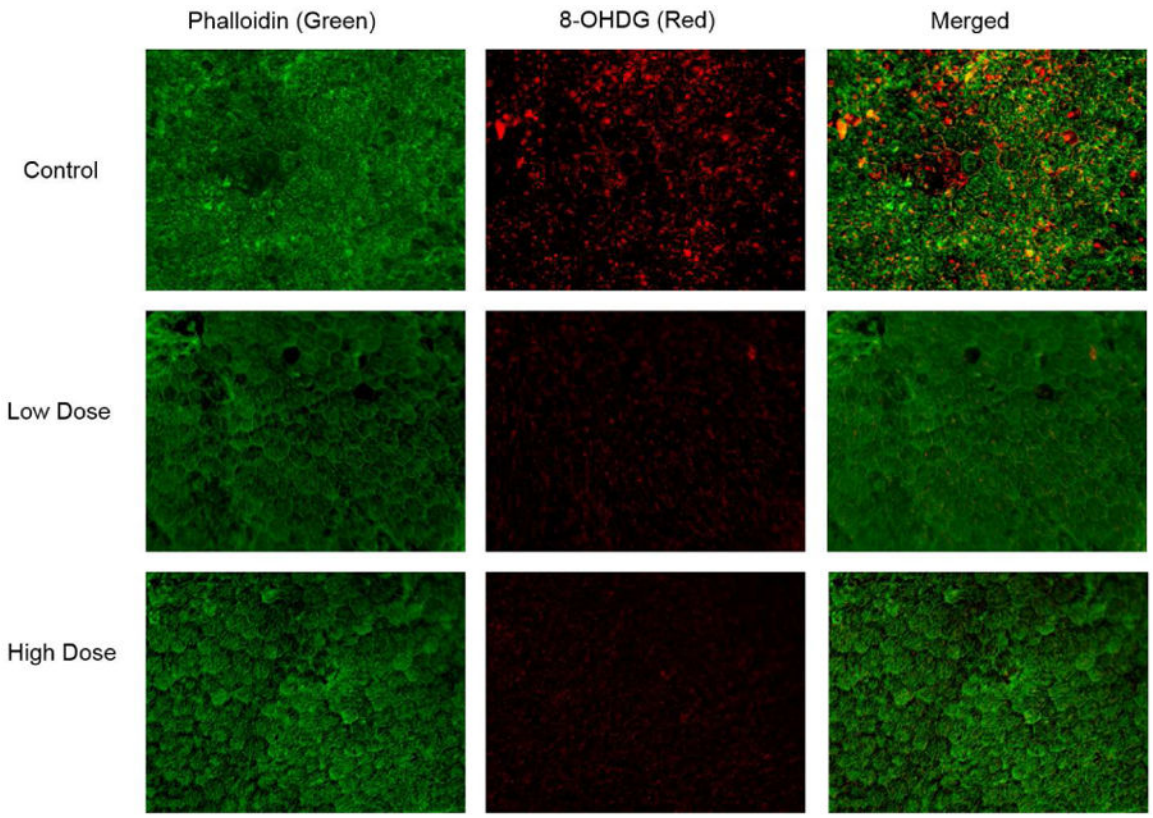

Fig. 5.

Treatment with 8-OH-DPAT reduces oxidative stress in the RPE. *Sod2*$^{flox/flox}$*VMD2-cre* mice were treated for one month by daily injection of saline (Control), 0.5 mg/kg of 8-OH-DPAT (Low Dose) or 5.0 mg/kg of 8-OH-DPAT (High Dose). They were then euthanized, enucleated and flat mounts were prepared from their RPE layers. These were stained with Alexa fluor 488 (green) conjugated phalloidin and with antibody to 8-OH-deoxyguanosine. The secondary antibody to detect 8-OH-dG was conjugated to Cy3 (red).

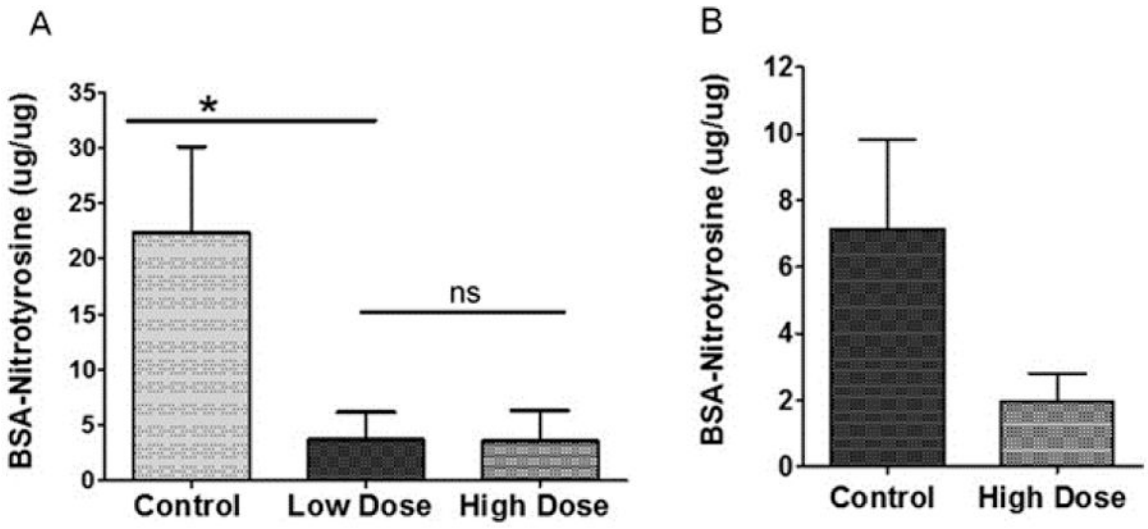

Fig. 6.

Treatment with 8-OH-DPAT reduces nitrotyrosine levels in the RPE of *Sod2*-deleted mice. *Sod2*$^{flox/flox}$*VMD2-cre* mice were treated for one month by daily subcutaneous injection of saline (Control), 0.5 mg/kg of 8-OH-DPAT (low dose) or 5.0 mg/kg of 8-OH-DPAT (high dose). Levels of nitrotyrosine modified proteins were measured using a competitive luminescence assay using a nitrated BSA standard curve. Assays were performed in duplicate from the indicated numbers of biological replicates. **A**. nitrotyrosine levels in RPE samples (n= 4 for high dose and control; n=5). **B**. nitrotyrosine levels in the retina (n=6 for the control, n=4 for the high dose). (We did not recover low dose retinas for this experiment.) (ns, not significant; *$p<0.05$). Error bars represent the standard deviation.

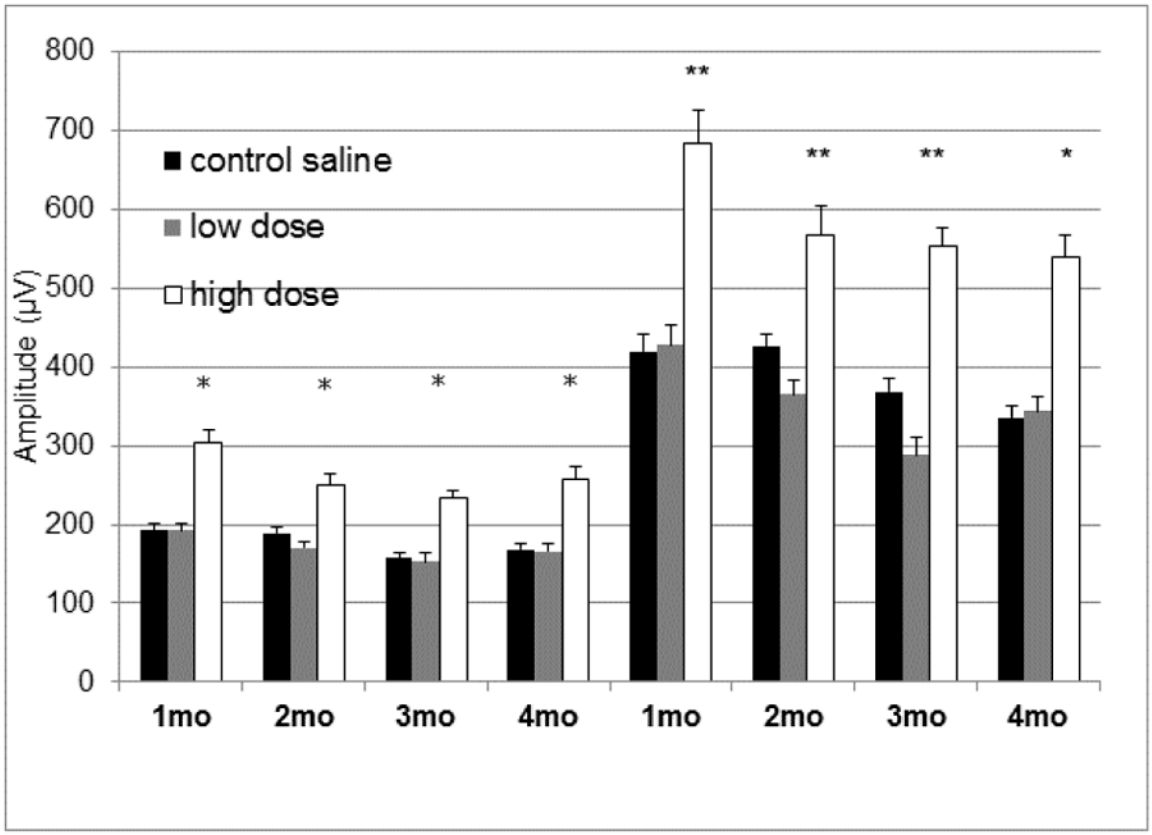

Fig. 7.

Treatment with high dose of 8-OH-DPAT leads to elevated scotopic ERG response. Dark-adapted electroretinogram responses were measured in doxycycline-induced *Sod2*$^{flox/flox}$*VMD2cre* mice at 1, 2, 3 and 4 months of age. The average a-wave amplitudes and the average b-wave amplitudes recorded at 0 dB (2.68 cds/m^2) flash intensity are shown. The same cohort of mice was used for all data points. For each time point 14 mice were used, except the 4 month time point at which n=11 (*$p<0.05$; **$p<0.01$). Error bars represent the standard error of the mean.

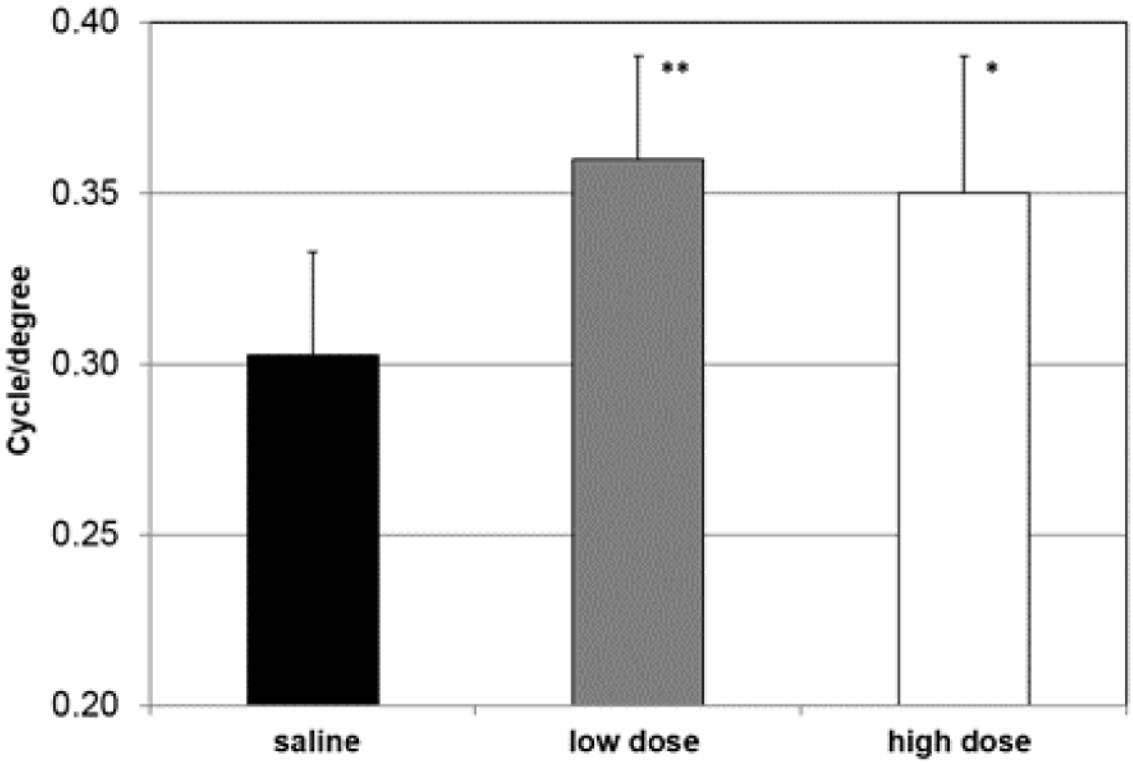

Fig. 8.

Visual acuity improves in 8-OH-DPAT treated mice. A. Mice were treated for four months with daily injections of saline or of 8-OH-DPAT at 0.5 mg/kg (low dose) or 5 mg/kg (high dose). Eight mice from each group were analyzed by Optomotry™ as described in the Materials and Methods. Error bands indicate standard deviation (* $p<0.05$; ** $p<0.01$).

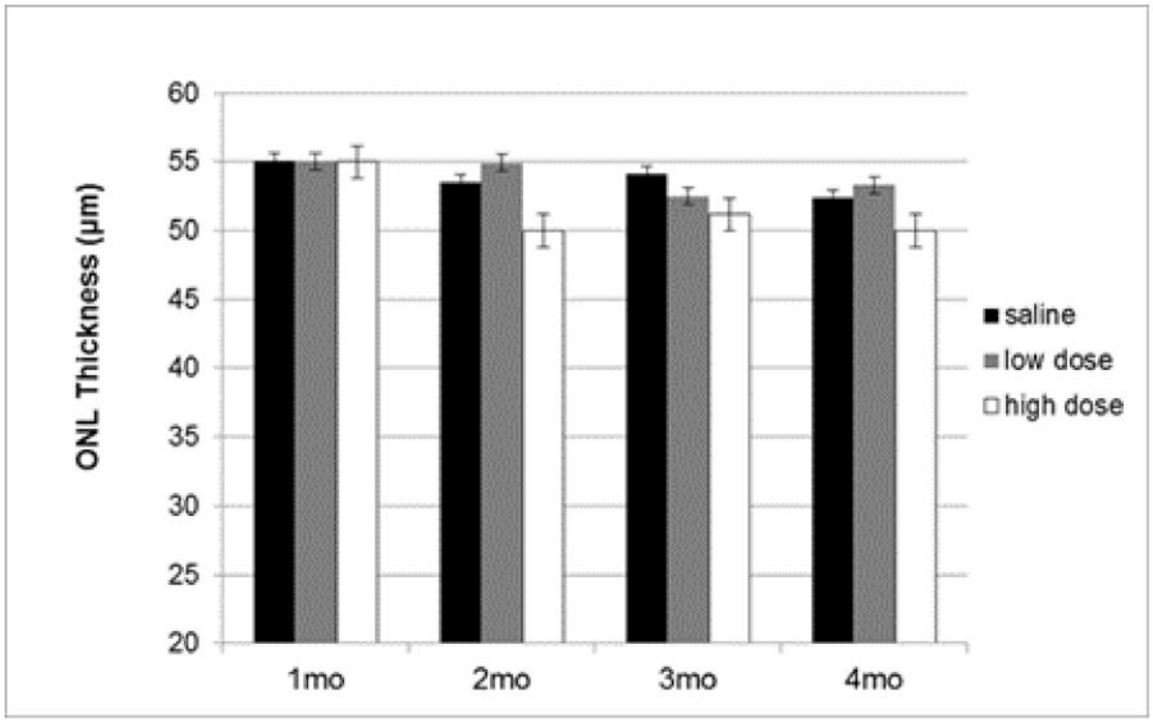

Fig. 9.

Drug treatment does not lead to increased ONL thickness. Thickness of the outer nuclear layer (ONL) was measured using SD-OCT between highly reflective lines indicating the outer plexiform layer and the external limiting membrane at four locations equally spaced from the optic nerve head. These values were averaged for each eye and then averaged for each age and treatment group (n=14 for months 1-3 and n=11 for month 4). The error bars signify standard error of the mean.

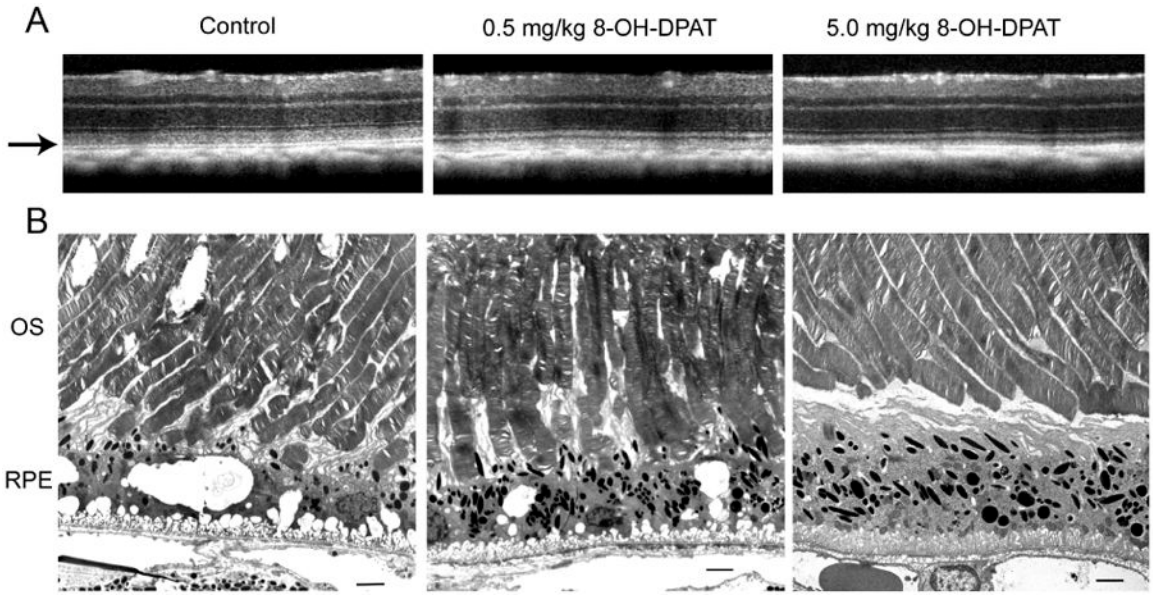

Fig. 10.

High dose 8-OH DPAT leads to improved architecture of photoreceptor outer segments and the RPE. Top SD-OCT images of retinas from the indicated treatment groups after four months of treatment (5 months of age). The arrow indicates the region of the photoreceptor outer segments. Electron micrographs of the outer segments and RPE from the same mice imaged by SD OCT. OS, outer segments; RPE, retinal pigment epithelium. The original magnification was 5000×, and the scale bar is 2 microns.

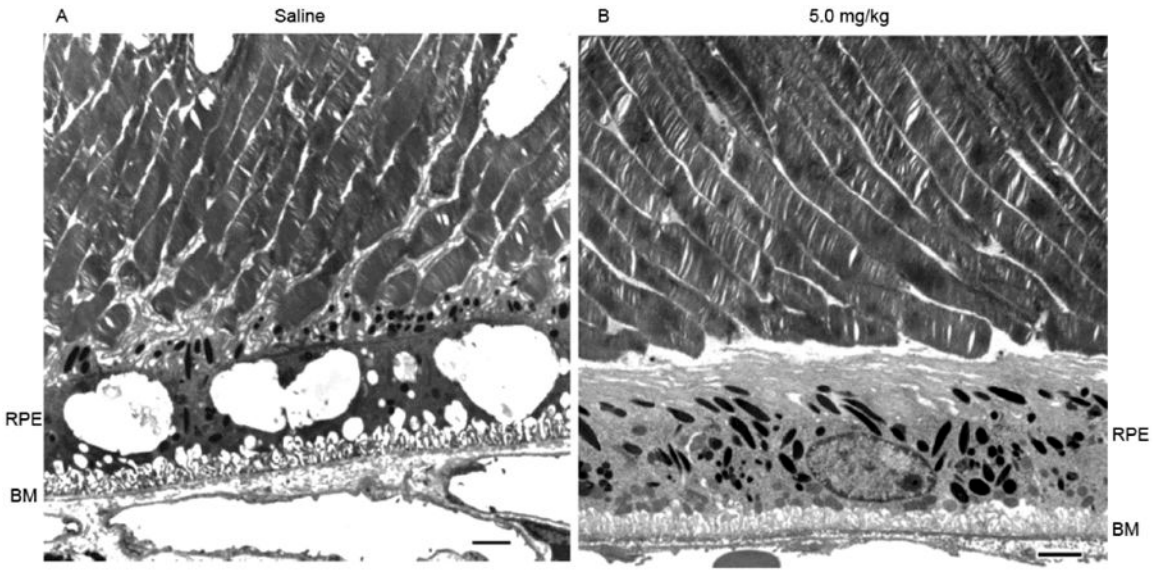

Fig. 11.

Treatment with 8-OH-DPAT reduces vacuolization in the RPE and stabilizes Bruch's membrane. Electron micrographs of the outer segment RPE interface from *Sod2* deleted mice treated with saline (A) or with 5 mg/kg of 8-OH-DPAT (B) for four months. Scale bar is 2 microns.

Table 1

Primers for PCR of antioxidant enzymes

Gene	Forward primer	Reverse primer
Murine		
Metallothionein 1	CCGGACTCGTCCAACGACTA	AGGAGCAGCAGCTCTTCTTG
Heme oxygenase 1	AGCCCCACCAAGTTCAAACA	GCAGTATCTTGCACCAGGCT
NqO1	CGACAACGGTCCTTTCCAGA	CCAGACGGTTTCCAGACGTT
SOD2	CAGGATGCCGCTCCGTTAT	TGAGGTTTACACGACCGCTG
Catalase	CAGCGACCAGATGAAGCAGTG	GTACCACTCTCTCAGGAATCCG
SOD1	TGCAGGGAACCATCCACTTCG	AACATGCCTCTCTTCATCCGC
β-actin	CGAGCACAGCTTCTTTGCAG	TTCCCACCATCACACCCTGG
Human		
Metallothionein 1	CGTGCGCCTTATAGCCTCTC	AGCAGCAGCTCTTCTTGCAG
Heme oxygenase 1	CCAGCGGGCCACAACAAAGT	GCCTTCAGTGCCCACGGTAAGG
NqO1	AAAGGACCCTTCCGGAGT AA	CCATCCTTCCAGGATTTGAA
SOD2	GTGTGGGAGCACGCTTACTA	AGAGCTTAACATACTCAGCATAACG
Catalase	GATAGCCTTCGACCCAAGCAAC	TGATTGTCCTGCATGCACATCG
SOD1	GTGCAGGTCCTCACTTTAATCCTC	ACCTTTGCCCAAGTCATCTGC
β-actin	AGCGAGCATCCCCCAAAG TT	GGGCACGAAGGCTCATCATT

NqO1, NAD(P)H dehydrogenase quinone 1; SOD2: superoxide dismutase 2; SOD1: superoxide dismutase 1.